IOP Conf. Series: Materials Science and Engineering **10** (2010) 012010 doi:10.1088/1757-899X/10/1/012010

Numerical Analysis for backside ground deformation behaviour due to braced excavation

Takahiro Konda[1], Hossain M Shahin[2] and Teruo Nakai[3]
[1]Assistant Manager, Geo-Analysis Group, Geo-Research Institute, JAPAN
[2]Associate Professor, Department of Civil Engineering, Nagoya Institute of Technology, JAPAN
[3]Professor, Department of Civil Engineering, Nagoya Institute of Technology, JAPAN

E-mail: konda@geor.co.jp

Abstract. Beam-spring model analysis is usually used as a practical design method for braced excavation in Japan. This method, however, has some limitations in large scale braced excavation, for example, sometimes observed wall displacement exceeds the design value in very soft and thick clay layer. In order to predict the influence of excavation process on ground deformation, it is necessary to employ numerical methods such as finite element method in which the interaction effects of soil and braced wall are taken into consideration. In this research 2D finite element analyses have been carried out for simulating a real field monitoring data of braced excavation. The observed data, design value computed from beam-spring model and the results of 2D FE analysis using an elasto-plastic constitutive model of soil (subloading t_{ij} model) are compared and evaluated in this paper. It is revealed that the analyses can properly capture wall displacement, surface settlement and deformation mechanism of the ground.

1. Introduction

In urban area, there are many underground structures constructed nearby by existing structures, which emphasis the necessity to construct the work safely to keep its influence on the surrounding structures to a minimum level. In design the main trend is to use empirical method [1] for the prediction of backside ground movement due to braced excavation. However, this method can explain a qualitative tendency of the ground deformation behaviour, and it can not predict the ground deformation quantitatively. There is a classical method where calculations are done separately, beam-spring model is used for the retaining wall and elastic FE analysis is used, applying the wall displacement, for getting the backside deformation. This method is troublesome and inconsequence to solve the braced excavation problem with the different prediction methods. In addition, an elastic FE analysis cannot consider the mechanical characteristics of soil appropriately, and it usually over estimates the deformed area of the ground. In this research, 2D finite element analyses using an elasto-plastic constitutive model of soils have been carried out for simulating a real field monitoring data of braced excavation [2] where the ground consists is very soft clay. The observed data [3], [4], design value computed from beam-spring model and the results of 2D FE analysis are compared and evaluated in this paper.

[1] 4-3-2, Itachibori, Nishi-ku, Osaka, 550-0012, JAPAN
[2,3] Gokiso-cho, Showa-ku, Nagoya, 466-8555, JAPAN

2. Soils characteristic and construction condition

2.1. Soils characteristic

Figure 1 shows the plan and cross-sectional view of ground in A-site which is considered in the calculation. Holocene layer and upper & lower Pleistocene layer exist from the ground surface to the place near the A-site. Holocene layer is composed of a fine sandy layer (1st aquifer) with 2m thickness having low *Uc* with SPT *N*-value equals to about 2, and a soft and sensitive clayey layer with SPT *N*-value = 0 - 3, I_L = 0.4 - 1.0, c = 20 - 100 kN/m^2. This Holocene clay layer is a typical soft it in this construction site. On the other hand, upper Pleistocene sandy and gravel layer Tsg (2nd aquifer) with partially scattered gravel, lower Pleistocene clayey layer Oc3 (c = about 400 kN/m^2) and lower Pleistocene sandy layer Os3 (3rd aquifer, SPT *N*-value >60) exist under the Holocene layer.

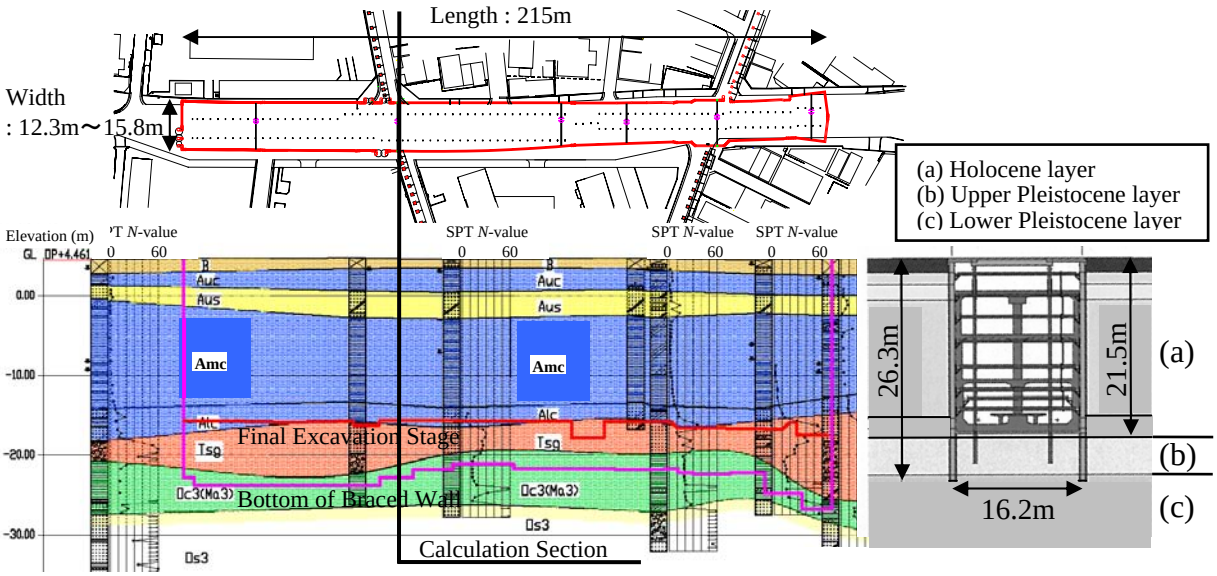

Figure 1. Plan and cross-sectional view of A-site.

2.2. Construction condition

Seepage control method was adopted in this construction site with extending the wall to the low permeable layer Oc3 (GL-26.3m). As the fluctuation of groundwater level is small which is about ±50cm, the drainage boundary of the backside ground is set as a steady water level in FE calculation. The excavation width was 16.2m and the final excavation depth was GL-21.5m. The Soil Mixing Wall is adopted for braced wall, and seven ties struts are installed with sequential striking construction method. Table 1 shows the detail specifications of the braced wall in A-site.

Table 1. Specification of braced wall in A-site.

Soil Mixing Wall (H-steel) condition						Excavation
Size (mm)		Pitch (m)	Length (m)	*EI* (kNm^2/m)	Area (m^2)	width (m)
H－588×300×12×20		0.6	26.3	399000	0.01872	16.248

Excavation Depth		Struts Depth		Struts Size	Span	Pitch	Area
Step	(GL-m)	Stage	(GL-m)	(mm)	*L* (m)	*S* (m)	*A* (m^2)
0th	1.506	Cover Beam	0.506	H－588×300×12×20	16.25	2.0	0.01872
1st	4.496	1st	3.496	H－300×300×10×15	14.76	2.5	0.01184
2nd	6.996	2nd	5.996	H－300×300×10×15	14.86	2.5	0.01184
3rd	8.696	3rd	7.696	H－300×300×10×15	14.66	2.5	0.01184
4th	11.196	4th	10.196	H－300×300×10×15	14.76	2.5	0.01184
5th	13.840	5th	12.840	H－350×350×12×19	14.46	2.5	0.01719
6th	15.950	6th	15.450	H－350×350×12×19	14.46	2.5	0.01719
7th	18.550	7th	18.050	H－350×350×12×19	14.46	2.5	0.01719
8th	21.550	—	—	—	—	—	—

3. Calculation condition

3.1. Process of FE Analysis

3.1.1. Constitutive Model of Soil

The finite element analyses have been carried out with FEM tij-2D software using an elasto-plastic constitutive model of soils, named subloading t_{ij} model [5]. The constitutive model requires a few soil parameters which can easily be obtained from conventional laboratory tests data. This model can consider influence of intermediate principal stress on the deformation and strength of soils, dependence of the direction of plastic flow on the stress paths, influence of density and/or confining pressure on the deformation and strength of soils.

3.1.2. Outline of FE analysis

Summary of ground constitutions and excavation details in finite element analysis are shown in Figure 2 and the finite element mesh is shown in Figure 3. The Amc layer is a thick and very soft clay layer which is a typical part in this construction site. Furthermore, as the grain size distribution of Amc layer is different in the vertical direction, Amc layer is modelled with three divided layer in FE analysis based on laboratory tests. The backside area from braced wall is extended to 4.5 times the excavation width to neglect the influences of boundary on the braced excavation based on the results of FE simulations changing the width of the ground. In the same way, the lower boundary is extended to GL-45m. The undrained boundary is set on the lower and side boundaries and the interface of wall. The drained boundary with free groundwater surface is set at GL-2m for steady condition. The excavation is carried out by deactivating the elements together with lowering the water surface in the excavation side. Therefore, after each stage of excavation the top surface is set as drained boundary in the excavation side. The wall is modelled as beam element. Joint element is used as an interface element between the wall and surrounding ground in both sides of the wall. The friction angle between the soil and wall is assumed as 20° when slippage is considered, and it is 90° when slippage is not considered. The struts are modelled with elastic supports considering the stiffness of the struts which are installed at different depths. FE analysis is carried out considering plane strain and soil-water coupled condition based on Akai & Tamura method [6].

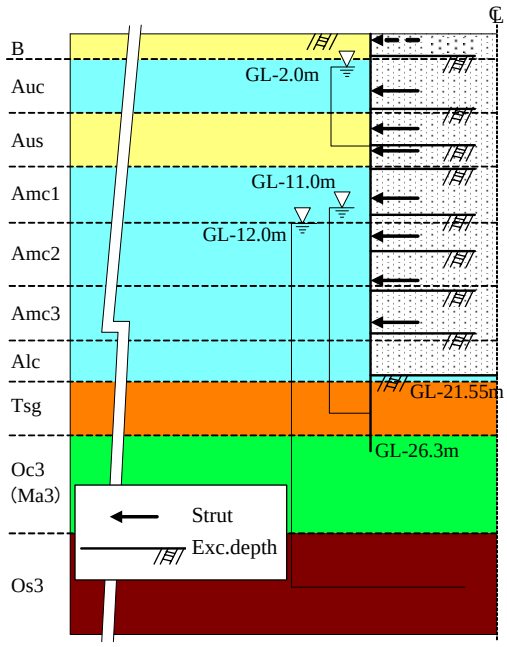

Figure 2. Ground constitutions and excavation details in FE analysis.

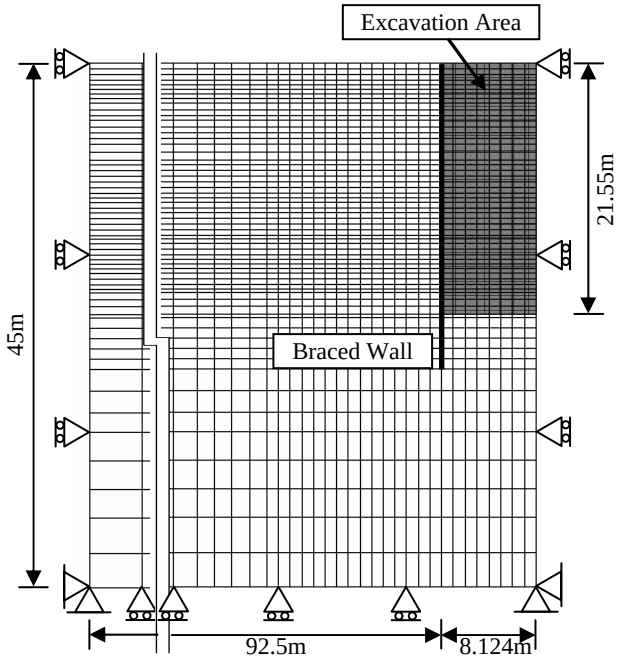

Figure 3. Finite element mesh.

3.1.3. Construction Process

Figure 4 shows the construction process in FE analysis. Consolidation period is considered in between two excavation stages for carrying material and installation of braced wall and some struts where necessary the same as the actual construction in the field. In this simulation, an average excavation speed against the total time of each construction stage is adopted. Moreover, the excavation is simulated by deactivating the elements of soil together with water adopting an average speed for each excavation stage.

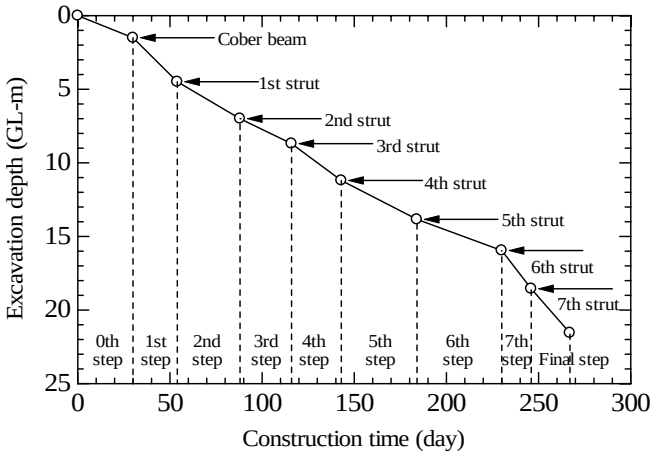

Figure 4. Construction process in FE analysis.

3.1.4. Initial Stress Condition

The initial stress in the ground is set to become a prescribed over consolidated ground by self-weight consolidation and uniform loading/unloading simulation from the bottom of the ground.

3.2. Determination of Soil Parameters

Soil parameters for elasto-plastic FE analysis is listed in Table 2. The results of element simulations for Aus, Amc1 and Amc3 layers, which are the typical layers of field ground of this construction site, are shown in Figures 5. The elements simulations against the laboratory Oedometer test and triaxial compression test are performed with axisymmetric condition the same as the laboratory tests. In the parameter lists, λ and κ denote the compression and swelling index, N means the void ratio at atmospheric pressure (p' = 98 kPa, q = 0 kPa) and R_{cs} is the principal stress ratio at critical state in triaxial compression. β represents the shape of yield surface and a denotes the influence of density and confining pressure. The detail meanings and the determination way of these soil parameters have been described in reference [5]. These parameters are soil material property and independent of the influence of density and/or confining pressure on the deformation and strength of soils.

Table 2. Soil parameters for elasto-plastic FE analysis (FEMtij-2D).

Layer		Lower Depth (GL-m)	SPT N-value (Time)	Unit weight γ_t (kN/m^3)	Soil parameters for elasto-plastic FE analysis (FEMtij-2D)							Permeability
					λ	κ	N	R_{cs}	β	a_{AF}	a_{IC}	k (cm/s)
Holo-cene	B	1.84	2	16.66	0.070	0.0045	1.10	3.20	2.00	30	500	1.67×10^{-5}
	Auc	4.94	4	16.66	0.16	0.02	1.23	2.10	1.30	500	500	1.67×10^{-7}
	Aus	8.34	2	16.66	0.07	0.01	0.68	3.50	1.50	200	100000	1.67×10^{-5}
	Amc1	12.00	0	15.68	0.16	0.02	1.23	2.25	1.57	40	500	
	Amc2	15.95	1	15.68	0.25	0.04	1.50	3.55	1.70	130	500	1.67×10^{-7}
	Amc3	19.44	4	16.66								
	Alc	21.84	6	17.15	0.14	0.02	1.05	3.55	1.10	30	500	
Pleisto-cene	Tsg	25.39	26	17.64	0.035	0.0023	1.10	3.20	2.00	30	500	1.67×10^{-5}
	Oc3	31.64	14	17.64	0.10	0.02	1.85	4.00	1.70	3500	500	1.67×10^{-7}
	Os3	45.00	84	19.60	0.007	0.0005	1.10	3.20	2.00	30	500	1.67×10^{-5}

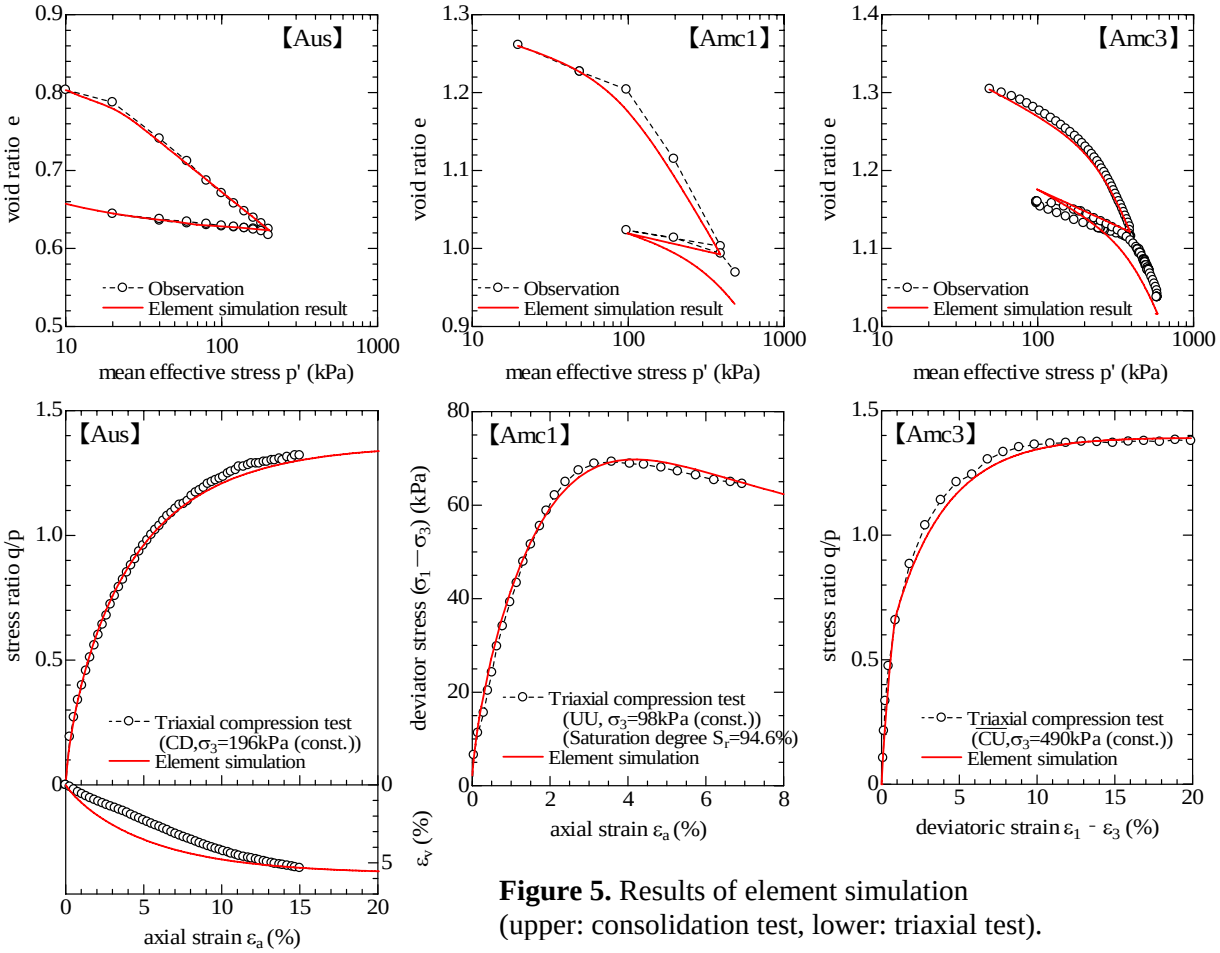

Figure 5. Results of element simulation
(upper: consolidation test, lower: triaxial test).

Here, some parameters of Amc3 clayey layer are obtained from the triaxial compression test ($\overline{\text{CU}}$ condition along the isotropic load/unload stress paths) taking undisturbed specimen from construction site. Other parameters clayey layers are estimated from the standard consolidation test and the triaxial compression test (unconsolidated-undrained condition) based on the foundation investigation data. In the element simulation of other clay layer, the sampling process and stress condition of real ground are regenerated. The compression of air in the sample is evaluated based on the Boyle's law after calculating the air void ratio from the degree of saturation in laboratory test to consider the compressibility of water in calculating the parameters of the soils. However, as the degree of saturation in the field was not measured in the field, in the elasto-plastic FE analysis the degree of saturation is assumed as 100%. Some parameters of Aus sandy layer are obtained from the triaxial compression test (CD condition along the isotropic load/unload stress paths) with reconstitution specimen fitting to the relative density in actual ground. Parameters of surface layer (B layer) are assumed as the same parameters of dense Toyoura sand [5]. Parameters of Tsg and Os3 layers are obtained fitting the stiffness with initial tangential line of stress-strain relation for dense Toyoura sand based on the coefficient of deformation predicted by average standard penetration test value [7]. Permeability of each layer is determined from consolidation and in-situ permeability tests.

4. Results and discussions

The observed data, design value computed from beam-spring model and the results of 2D elasto-plastic FE analysis are compared and evaluated focused on the braced wall deflection and backside ground movement due to braced excavation. Besides the finite element analysis, the frame analysis with beam-spring model is conducted to calculate the design value. The layout of the frame analysis [8] is shown in Figure 6.

4.1. Braced wall deflection

Figure 7 shows the comparison of braced wall deflections among observations, FE analysis results and design values obtained from frame analysis. Here, slippage of interface elements between beam elements of braced wall and solid elements of soil is considered assuming frictional angle $\delta = 20°$. It is seen in the figure that the observed wall displacement increases with the progress of braced excavation, and the peak value of displacement appears at the bottom of each excavated layer till the 5th excavation stage, after the 5th excavation stage it appears at the upper side of excavation. Moreover, the maximum braced wall displacement is about 2cm due to the excavation of Aus layer in the 3rd excavation stage, on the other hand, the braced wall deflection increases to about 5.5cm due to the excavation of alluvial soft clay layer in the final excavation stage.

The wall displacement of FE analysis increases with the progress of braced excavation, too. However, the displacement value in FE analysis is larger than the observed one till the 3rd excavation stage. One of the reasons of this tendency might be the underestimation of the strength and deformation characteristic in B, Auc and Aus layers. However, in the final excavation stage, the maximum wall deformation and its location of FE analysis are very similar with the observed data. On the other hand, the design value of maximum wall displacement is smaller than the observed one, and its location is above the measured depth. As the observed wall displacement is larger than the design value for deeper excavation stages, the frame analysis of braced excavation underestimates the wall displacement. It can be said that the FE analysis can predict the amount and distribution of wall displacement during the braced excavation appropriately.

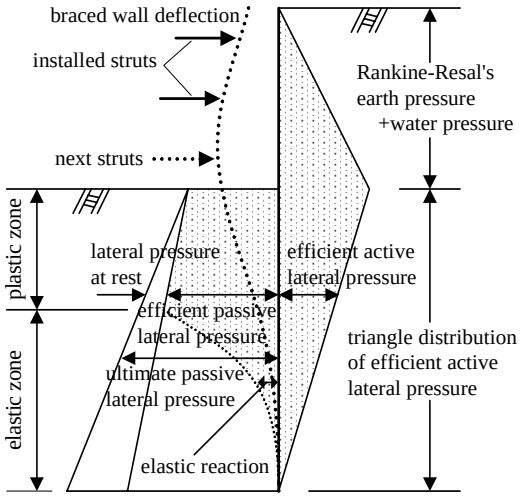

Figure 6. Outline of frame analysis for braced excavation [8].

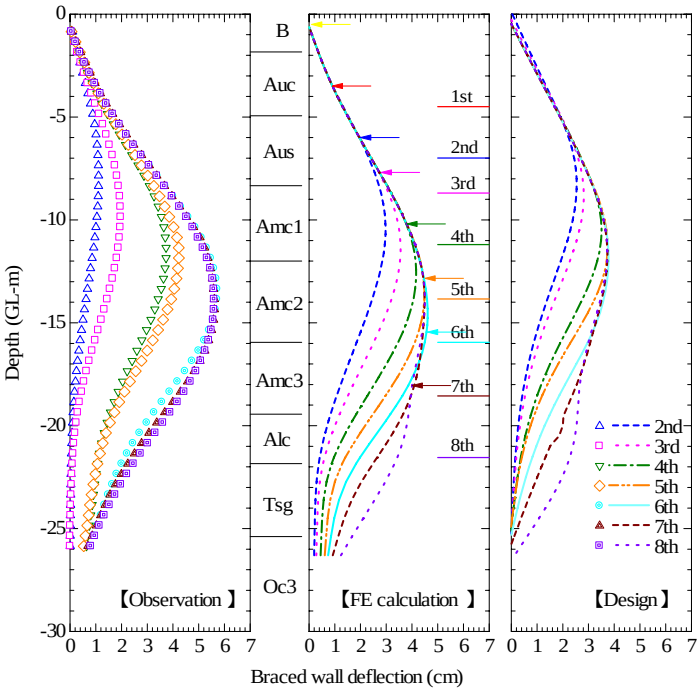

Figure 7. Comparison of braced wall deflections.

4.2. Backside ground surface settlement

Figure 8 shows the profiles of the backside ground surface settlement for each excavation stage. Abscissa represents the distance from the braced wall towards the back side where “0” on the right edge corresponds to the position of the braced wall. The magnitude of the backside ground surface settlements are compared and examined among some monitoring data and the results of the FE simulations, as backside ground settlement can not be obtained directly by the frame analysis. It is seen that the settlement of the ground adjacent to the braced wall is restrained due to the friction effects between the braced wall and surrounding ground. The settlement gradually increases with the

distance from the braced wall until a distance of about 9m where the maximum settlement occurs beyond which it decreases and finally ceases at a distance of about 30m from the braced wall in the field observation. The magnitude of the maximum settlement is about 2.5cm. It is also seen that U-shaped settlement troughs is formed due to the braced excavation. Similar to the observed data finite element analysis shows U-shaped settlement troughs, though the maximum settlement which is about 3.5cm and its location (about 10 to 13m from the braced wall depending on the excavation stage) are slightly over-predicted compared to the observed ones. Here, it is noted that the location of the maximum settlement gradually moves away from the braced wall with the advancement of the excavation. Moreover, in the finite element analysis the width of the settlement trough is wider than that of the field observation. However, a uniform distribution of settlement is seen at distance of 50 to 70m from the braced wall in the simulations.

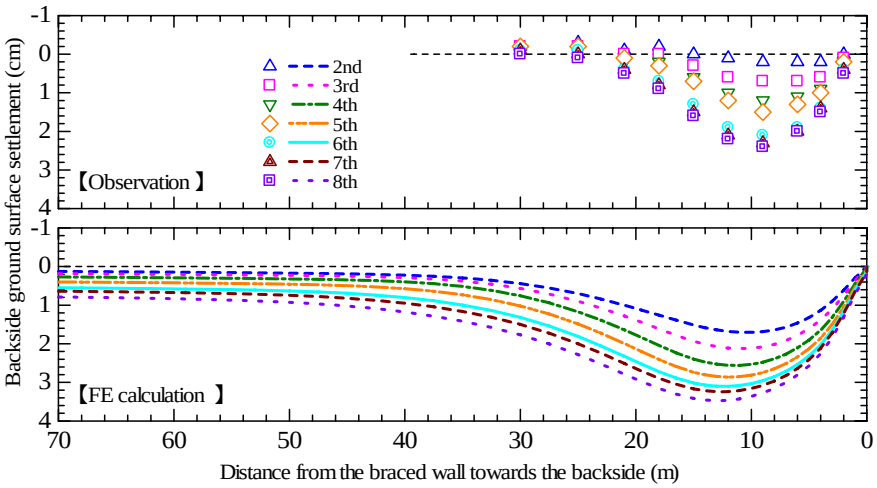

Figure 8. Comparison of backside ground surface settlement profiles.

4.3. Backside ground deformation behavior

Figure 9 shows the distribution of braced wall displacement, backside ground displacement vectors and surface settlement profiles of the field observation. In the field, movements of the ground were captured in section No.1 which is about 2m and in section No.2 which is about 9m away from the braced wall. The maximum wall deflection was 38mm at the middle of Amc layer (GL-12.5m). Due to the wall deflection the maximum horizontal ground displacement in section No.1 was about 29mm at the location slightly above the maximum deformation depth of the wall. On the hand, the maximum horizontal ground displacement in section No.2 was about 12mm in between Auc layer and Aus layer. It is seen that the wall deflection caused the back side ground deformation similar to circular slippage and this influence reached to the ground surface. The deformation of the back side ground is seen mainly in the area bounded with the lines projected in the directions of 45° to 60° from the bottom of braced wall, which is usually used in common practice. Therefore, the result is consistent with the commonly seen in the field observation. The 60° line shows the area of an active earth pressure zone approximately.

Figure 10 shows the ground displacement vectors in the end of last excavation stage obtained from the FE simulation. The intensity of the ground deformation is displayed according to colour group as shown in explanatory notes. The simulation results are resemblance to the field observation although the area of the ground deformation of the back side is a little wider than field observation. From these above-mentioned discussions it can be said that the elastoplastic FE analysis can predict the phenomenon of the back fill ground deformation in the braced excavation problem adequately.

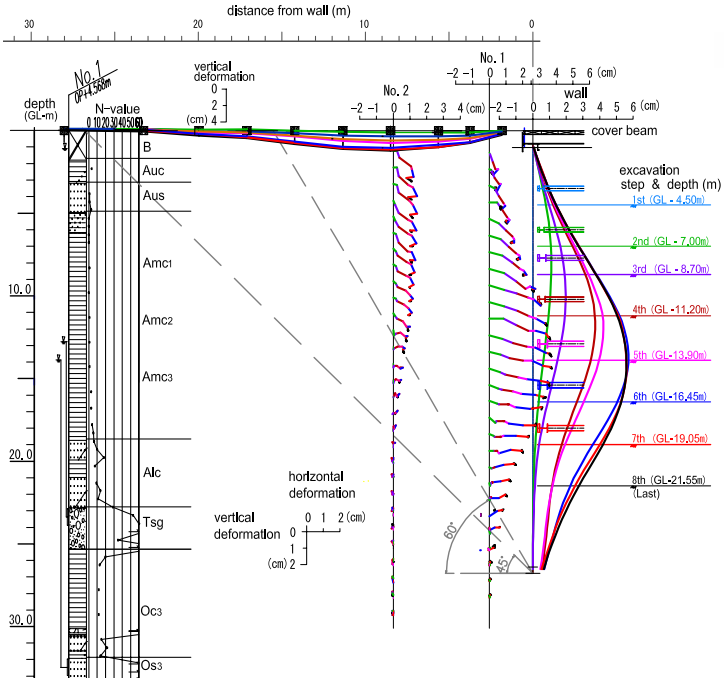

Figure 9. Backside ground movement phenomenon (observed data).

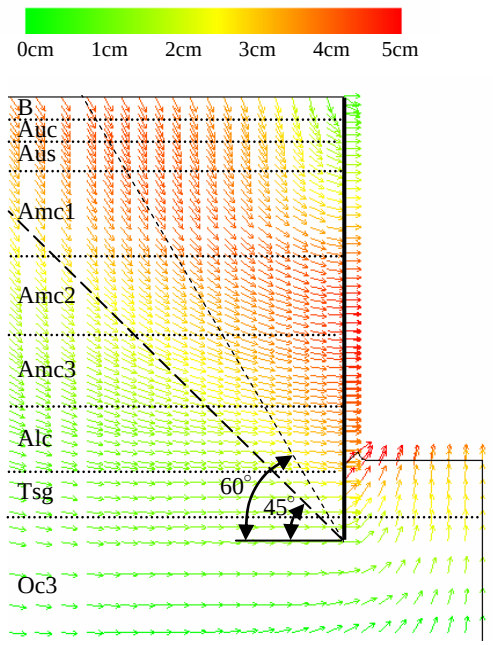

Figure 10. Ground displacement vectors (results of FE simulation).

5. Parametric studies considering deferent ground characteristics

A simple method for the prediction of the back ground surface settlement is rotating the deformation of the braced wall to the back side by 90°. However, it is well known that the ground deformation is different for different soil property. Here, the elastoplastic FE analysis is employed in the different soil conditions for the estimation of different tendency such as the amount of the maximum settlement, location of the maximum settlement and the shape of the settlement troughs [9].

5.1. *Conditions of Parametric Study*

Some parametric numerical analyses are executed for several soil conditions whose parameters are listed in Table 3. Here, the initial void ratio of S1 and S2 layer is estimated from the relative density Dr = 20% and Dr = 90%. Normally consolidated clay (OCR = 1) is assumed in C1 layer. The drain condition is set in sandy layer and the undrained condition is set in clayey layer for the drainage boundary. The interface between the braced wall and surrounding ground is considered as rigidly connected (the friction angle of the braced wall $\delta = 90°$). The initial stress is analyzed as isotropic condition. Furthermore, an elastic FE analysis (Case 4) is employed to compare the results with the elastoplastic FE analysis. The Young's modulus for elastic analysis is obtained from the stress and strain relation of one element simulation taking the value of E_{50}.

5.2. *Results of Parametric Study*

The distribution of the backside ground surface settlement at the end of the excavation for CASE 1 is shown in Figure 11(c). In addition, the observed braced wall displacement is added in all cases. It is revealed that the stiffer ground produces smaller amount of the maximum settlement and volume of total settlement. On the other hand, the looser ground produces a sharper curvature of settlement distribution close to the braced wall. The elastic FE analysis (CASE 4) results a wider area of surface settlement and the distribution of settlement has a different tendency compared with elastoplastic FE analyses results, which is an obvious case. Figure 11(d) shows the distribution of settlement for each case at the end of the excavation. The vertical axis denotes a non-dimensional value in which the

settlement of each node is divided with the maximum value. In CASE 1 where the ground only consists with sandy layers, the maximum settlement occurs locally very close to the braced wall and U-shaped settlement trough is formed in this case. On the other hand, in CASE 2 where a normally consolidated clay layer exists in between sandy layers, the location of the maximum settlement is far from the braced wall compared to CASE 1, and the influence of the excavation extends in a wider region. In CASE 3 where the ground consists with only normally consolidated clay layers, the above tendency is more distinguished. Therefore, different soil properties the location and the amount of the maximum settlement are different, which changes the range and shape of settlement troughs as well. Comparing the results of elastic FE analysis, where the distribution of surface settlement expands in a wider region, with the results of the elastoplastic analyses the necessity of elastoplastic analysis can easily be comprehended.

Table 3. Soil parameters and formation of soil layer for parametric analyses.

Layer	Unit weight γ_t (kN/m^3)	Soil parameters for elasto-plastic FE analysis (FEMtij-2D) λ	κ	N	R_{cs}	β	a_{AF}	a_{IC}
S1	16.66	0.070	0.0045	1.10	3.20	2.00	30	500
S2	19.60							
C1	16.66	0.104	0.0099	0.92	3.20	1.50	50	500

① : B ② :Auc ③ :Aus ④ :Amc1 ⑤ :Amc2 ⑥ :Amc3 ⑦ :Alc ⑧ :Tsg ⑨ :Oc3 ⑩ :Os3

CASE 1	①～⑦	S1	CASE 2	①～③	S1	CASE 3	①～⑦	C1	CASE 4	①～⑦	S1 (E_{50}=234 MN/m^2)
	⑧～⑩	S2		④～⑦	C1		⑧～⑩	S2		⑧～⑩	S2 (E_{50}=320 MN/m^2)
				⑧～⑩	S2						

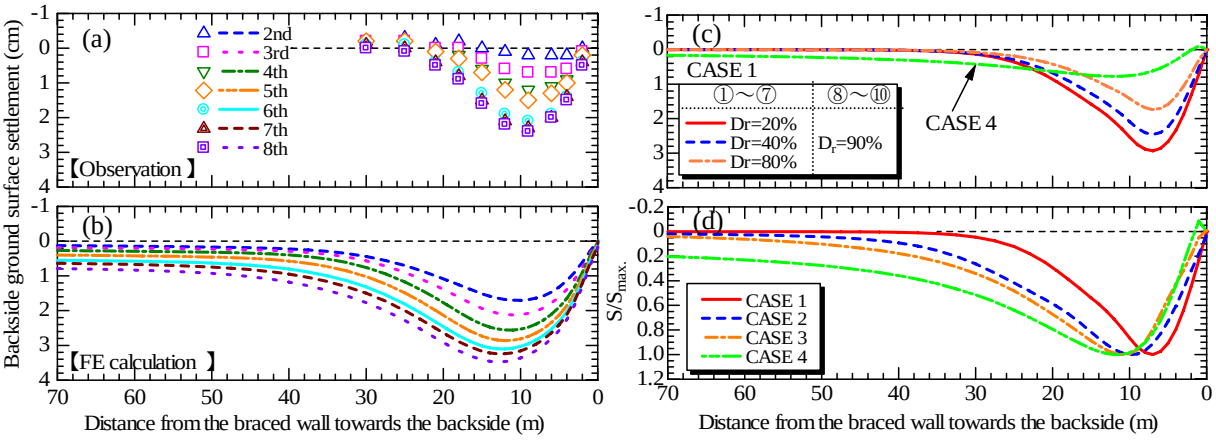

Figure 11. Comparison of backside ground surface settlement.

6. Conclusions

In a usual braced excavation problem, the braced wall displacement and the ground movement are often separately predicted. In this research, to predict the stress and deformation behaviour of the ground due to braced excavation from the same viewpoint, the elastoplastic FE analysis which can properly consider the mechanical characteristic of soil material and the construction process and the interaction between existing structures and surrounding ground is employed on the braced excavation where the soft clay ground exists. The braced wall displacement and backside ground deformation are compared and evaluated between calculation results, monitoring data and design value. Moreover, the FE analysis with subloading t_{ij} model is examined about the applicability for actual construction site. The results can be concluded as follows;

(1)The results of elastoplastic FE analysis have a good correspondence with the observed data in the cases of the maximum displacement, the initiation depth of it and the deflection of the wall in the final excavation stage.
(2)The U-shaped settlement trough is seen in the backside ground surface and there is a good correspondence in the amount of the maximum settlement and the location of occurrence between the calculation results and monitoring data. However, the area of settlement of the back side ground in the calculation is wider than the observed data.
(3)The deformation of the back side ground is seen mainly in the area bounded with the lines projected in the directions of 45° to 60° from the bottom of braced wall. Though the calculated backside ground movement is a little larger than the observation, the elastoplastic FE analysis can predict the phenomenon of the field observation.
(4)The backside ground surface settlement due to braced excavation occurs near the braced wall locally and narrower settlement area is seen in sandy ground. On the other hand, surface settlement spreads to a far distance gently in normally consolidated clayey ground. Herewith, even if the braced wall displacement is same, the distribution of surface settlement varies with the properties of soil. Moreover, this tendency is obviously different according to the difference of the constitutive model of the soils.

The parameters of the elastoplastic constitutive model named subloading t_{ij} model can easily be obtained from conventional laboratory tests data uniquely without depending on the density and/or confining pressure on the deformation and strength of soils. Therefore, the FE analysis, where construction process and soil mechanical characteristics are properly considered, can reproduce the stress and deformation behaviour of a ground comprehensively due to actual braced excavation.

7. References

[1] Peck, R. B. 1969 Deep excavation and tunnelling in soft ground *Proc. 7th ICSMFE State of the Art Report 1* 225-290
[2] Konda, T., Hossain M. Shahin and T. Nakai 2009 Elasto-plastic finite element analysis for the deformation behaviour of ground due to braced excavation *JSCE Journal of Geotechnical and geoenvironmental engineering* **65** 1 213-225 in Japanese
[3] Ito, H., T. Yanagawa, T. Konda and K. Hayakawa 2006 Relation between braced wall deflection and deformation behaviour of backside ground due to braced excavation *The Proc. of Tunnel engineering JSCE* **16** 439-446 in Japanese
[4] Konda, T., Ota, H., Yanagawa, T. and Hashimoto, A. 2008 Measurements of ground deformations behind braced excavations *The Proc. 6th Int. Symposium Geotechnical Aspects of Underground Construction in Soft Ground (IS-Shanghai)* 295-300
[5] Nakai, T. and Hinokio, M. 2004 A simple elasto-plastic model for normally and over consolidated soils with unified material parameters *Soils and Foundation* **44** 2 53-70
[6] Akai, K., and T. Tamura 1978 Numerical analysis of multi-dimensional consolidation accompanied with elasto-plastic constitutive equation *JSCE Journal of Geotechnical and geoenvironmental engineering* **269** 95-104 in Japanese
[7] Architectural Institute of Japan 1988 Recommendations for design of building foundation 152-154
[8] Osaka Municipal Transportation Bureau 1993 Design Guideline for temporary structure (draft) in Japanese
[9] Konda, T., Hossain M. Shahin and T. Nakai 2009 Numerical analysis for backside ground surface settlement of braced wall considering the deference of ground character *Proc. of the 44th JNCSFE* 1039-1040 in Japanese

Numerical analysis for backside ground deformation behaviour due to braced excavation

2010 IOP Conf. Ser.: Mater. Sci. Eng. 10 012010

(http://iopscience.iop.org/1757-899X/10/1/012010)